increase of the probability of outage events is needed, and can be obtained with a high T. In this cases, the method is practically reduced to the standard MC.

5. CONCLUSIONS

A novel approach to the evaluation of the outage probability of compensated systems through simulations has been proposed. It is based on a MC integration applied to Markov chains (MCMC) and is very fast and accurate. An excellent agreement with a recently proposed analytical method [2] has been demonstrated for first-order compensated systems, both proving the accuracy of MCMC and extending the validity of [2] down to very low values. With respect to the analytical method, the proposed MCMC is based on an all-orders PMD model and can be used regardless of the complexity of the PMD compensator. Moreover, with respect to standard MC, it allows a fast and accurate evaluation down to extremely low values. Finally, with respect to iterative MC procedures, such as MMC, it is based on a one-shot MC integration and on the straight evaluation of $P(\mathcal{O})$, without the need of an histogram-based pdf estimation, and without any problem related to the stability of the iterative procedure. Thus, the accuracy of the method can be increased at will. A procedure for the continuous monitoring of the uncertainty has been described as well, allowing to stop the integration when the desired accuracy is reached.

REFERENCES

[1] H. Bülow, "System outage probability due to first- and second-order PMD," *IEEE Photon. Technol. Lett.*, vol. 10, pp. 696–698, May 1998.

[2] E. Forestieri and G. Prati, "Exact analytical evaluation of second-order PMD impact on the outage probability for a compensated system," *J. Lightwave Technol.*, vol. 22, pp. 988–996, Apr. 2004.

[3] S. L. Fogal, G. Biondini, and W. L. Kath, "Multiple importance sampling for first- and second-order polarization-mode dispersion," *IEEE Photon. Technol. Lett.*, vol. 14, pp. 1273–1275, Sep. 2002.

[4] A. O. Lima, J. I. T. Lima, J. Zweck, and C. R. Menyuk, "Efficient computation of PMD-induced penalties using multicanonical monte carlo simulations," in *Proc. ECOC'03*, 2003. Paper We3.6.4.

[5] J. C. Spall, "Estimation via Markov chain Monte Carlo," *IEEE Contr. Syst. Mag.*, pp. 34–45, Apr. 2003.

[6] N. Metropolis, A. W. Rosenbluth, M. N. Rosenbluth, A. H. Teller, and E. Teller, "Equation of state calculations by fast computing machines," *J. Chem. Phys.*, vol. 21, no. 6, pp. 1087–1092, 1953.

[7] W. K. Hastings, "Monte Carlo sampling methods using Markov chains and their applications," *Biometrika*, vol. 57, pp. 97–109, 1970.

[8] E. Forestieri, "Evaluating the error probability in lightwave systems with chromatic dispersion, arbitrary pulse shape and pre- and postdetection filtering," *J. Lightwave Technol.*, vol. 18, pp. 1493–1503, Nov. 2000.

A PARAMETRIC GAIN APPROACH TO PERFORMANCE EVALUATION OF DPSK/DQPSK SYSTEMS WITH NONLINEAR PHASE NOISE

P. Serena, A. Orlandini, and A. Bononi

Università degli Studi di Parma, Dipartimento di Ingegneria dell'Informazione

Parco area delle scienze 181/A, 43100 Parma (Italy)

serena@tlc.unipr.it

Abstract: We present a novel method based on parametric gain (PG) to study the impact of nonlinear phase noise in dispersion-managed differentially phase-modulated optical transmission systems. By linearizing the interaction of signal and noise, the received ASE is approximated as a stationary Gaussian process, whose statistics are found by using a low-pass filtered version of the modulating signal. The BER is then evaluated by adapting standard methods for quadratic detectors, for single-channel binary and quaternary PSK systems, both for NRZ and RZ supporting pulses. We show that in the RZ case parametric gain causes a larger penalty than in the NRZ case, and that DQPSK is less robust to PG than DPSK.

Key words: phase noise; differential phase-shift keying (DPSK); differential quadrature phase-shift keying (DQPSK); parametric gain; Gaussian noise.

1. INTRODUCTION

Optical phase shift keying (PSK) modulation formats are an interesting alternative to on-off keying (OOK) for long-haul transmission systems, because of their lower optical signal-to-noise ratio (OSNR) requirements, which leads to reduced power and thus reduced Kerr nonlinearities. PSK formats are usually implemented as differential binary (DPSK) or quaternary (DQPSK) schemes [1, 2]. DPSK encodes the information onto the differential optical phase between adjacent bits which can be either 0 or π, while DQPSK utilizes two orthogonal DPSK signals, which leads to four possible values of the differential phase $0, \frac{\pi}{2}, \pi, \frac{3}{2}\pi$, thus doubling spectral efficiency. However, PSK formats are extremely vulnerable to nonlinear phase noise [3] arising by the nonlinear interaction of signal and amplified spontaneous emission (ASE) noise during propagation. Such an interaction manifests itself also as a parametric gain (PG) of the received ASE noise. It has been experimentally shown

that, in 10 Gb/s DPSK systems, the statistics of the decision variable in presence of nonlinear phase noise develop a much larger skewness than without nonlinearity, and resemble an exponential distribution [1]. Attempts have been made to theoretically study the statistics of the nonlinear phase noise (and an exact expression has been found only at zero group-velocity dispersion (GVD) [4]), in order to assess the performance of DPSK receivers based on ideal phase discriminators.

In this work we instead address the performance of realistic PSK receivers based on Mach-Zehnder delay demodulators. Although the statistics of the signal-inflated ASE noise depart from Gaussian at either very large signal levels or at zero GVD, we first show that in practical systems, working at sufficiently large OSNR and in which some local GVD is present, the received ASE noise can still be reasonably described by a Gaussian process.

While with non-return to zero (NRZ) supporting pulses the intensity is constant and the received ASE is a stationary process, in presence of return-to-zero (RZ) pulses the ASE parametric gain becomes time dependent, and thus the ASE is a non-stationary process. The exact non-stationary statistics of the ASE can in principle be obtained through a computationally heavy method based on the linearized solution of the nonlinear Schrödinger equation (NLSE) [5]. In this work, we find instead an *equivalent* stationary ASE process yielding the correct statistics of the decision variable. The bit-error rate (BER) is finally evaluated by a suitable modification of well-established methods for quadratic detectors in Gaussian noise [6].

We apply our model to provide a comparative study of the performance of single-channel dispersion managed DPSK and DQPSK systems, both for NRZ and RZ supporting pulses. Results are provided in terms of OSNR penalties for different system bitrates, in-line residual dispersion and cumulated nonlinear phase.

2. SYSTEM SET-UP

In Fig. 1 we schematically describe the single channel dispersion-managed DPSK multi-span system studied in the following sections. Before and after the transmission link, pre- and post- compensating fibers are optimized in presence of PG for each launched power value, while all spans have identical residual dispersion, varied in a suitable range at different bitrates. The receiver has an optical Gaussian filter of bandwidth $B_0 = 1.8R$, being R the system bitrate, followed by a Mach-Zehnder interferometer with one bit delay equal to $T = 1/R$. Half the sum of the input fields at times t and $t - T$ is detected by one photodetector, while half the difference is detected by the other. The difference between the received currents is then filtered by a Butterworth 2nd order filter, of bandwidth $B_e = 0.65R$, and finally sampled. For the DQPSK

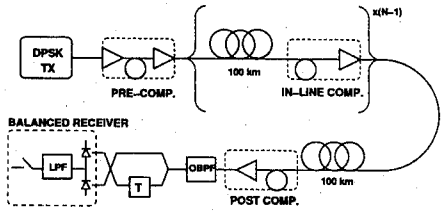

Figure 1. Set-up of the single channel dispersion managed DPSK system.

format, we consider two independent DPSK demodulators for the detection of the in-phase and quadrature signal components, with an additional delay of $\pi/4$ and $-\pi/4$ in each of the Mach-Zehnders [2]. We approximate the DQPSK in-phase and quadrature components as independent random variables (RVs), so that the BER is the average between the BER on each of such components.

3. ASE STATISTICS

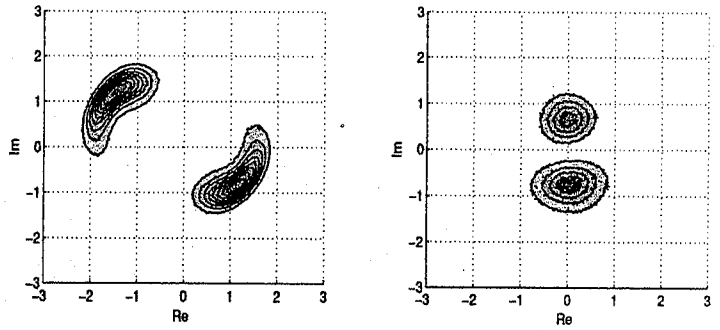

Figure 2. Contour plots of ASE PDF before the receiver for OSNR=25 dB, $\Phi_{NL} = 0.3\pi$ rad and $D_{tx} = 0$ ps/nm/km (left) or $D_{tx} = 4$ ps/nm/km (right).

It is known that signal and ASE have maximum nonlinear interaction strength at zero GVD, so that in such a case the received ASE has statistics far from Gaussian. We estimated the joint probability density function (PDF) of the in-phase (real) and quadrature (imaginary) received ASE components through a Monte Carlo simulation of a single fully-compensated fiber span with an NRZ-DPSK signal (see Fig. 1) operating at a received OSNR of 25 dB (over 0.1 nm), with a transmission fiber chromatic dispersion D_{tx} equal to either 0 or 4 ps/nm/km and for an average cumulated nonlinear phase $\Phi_{NL} = 0.3\pi$ rad. At $D_{tx} = 0$ we obtained the joint PDF contour levels shown in Fig. 2 (left), which confirm that Kerr nonlinearity alone causes a non Gaussian ASE. When

which have an elliptical shape, typical of a Gaussian bivariate distribution. We conclude that even a small amount of fiber GVD tends to reshape the ASE joint PDF towards a Gaussian distribution, provided that the OSNR is sufficiently large. Being the single span a worst case for the Gaussian assumption, such a conclusion holds also for multiple spans, where the increased number of independent noise sources accelerates the convergence to a Gaussian PDF.

4. MODEL FOR NOISE PROPAGATION

In this section we calculate the ASE noise statistics starting from a linearized solution of the NLSE [5] applied to long *periodic* dispersion-managed systems. For such systems the local dispersion is a z-periodic function, being z the distance, which can be written as $D_c(z) = \langle D_c \rangle + L^{-1}\Delta D_c(z/L)$, where $\langle D_c \rangle$ is the span-averaged dispersion, i.e. the in-line residual dispersion per unit length, and $L^{-1}\Delta D_c(z/L)$ is the local deviation from the average, with L equal to the single span length. In this context, the dynamic behavior of the propagating field can be described by a "slow" length scale z and a "fast" scale z/L, which allows to study the NLSE by a multiple scale approach [7].

First, let us assume the transmitted signal to be a continuous wave (CW). By writing the NLSE in terms of its characteristic lengths and exploiting the multiple scale method, we obtain that the noise field $a(z,\omega)$ propagates as:

$$\frac{\partial a(z,\omega)}{\partial z} = + \; j\,\mathrm{sgn}\left(\langle D_c \rangle\right)\frac{\omega^2}{2L_D}a(z,\omega) - \; j\frac{1}{L_{NL}}\cdot\frac{L_A}{L}\left[a(z,\omega)+\frac{a^*(z,-\omega)}{1-j\frac{L_A}{L_\Delta}\omega^2}\right]+S(z,\omega) \quad (1)$$

where $L_D = (2\pi c/\lambda^2)\,T_m^2/\left|\langle D_c \rangle\right|$ is the span-averaged dispersion length, being λ the signal wavelength and T_m the supporting pulse duration. The differential dispersion length $L_\Delta = (2\pi c/\lambda^2)\,T_m^2/(D_{tx} - \langle D_c \rangle)$ accounts for the deviation of the dispersion length $L_d = (2\pi c/\lambda^2)\,T_m^2/\left|D_{tx}\right|$ of the transmission fiber from the span average value, i.e. $1/L_d = 1/L_D + 1/L_\Delta$. L_A is the attenuation (or effective) fiber length, L_{NL} is the transmission fiber nonlinear length, proportional to the inverse of the signal power P. All the dispersive lengths are referred to $T_m = d \cdot T$, being d the signal duty-cycle, and ω is the frequency normalized to $1/T_m$. $S(z,\omega)$ is a Langevin Gaussian forcing term with autocorrelation at times t_1, t_2 equal to $\langle S(z_1,t_1)\,S^*(z_2,t_2)\rangle = \sigma^2\delta(z_1-z_2)\,\delta(t_1-t_2)$, where σ^2 is the white ASE power spectral density (PSD) per unit length and $\delta(\cdot)$ is the Dirac delta function. Eq. (1) is a linear differential equation with constant coefficients which can be cast in closed form in terms of a matrix exponential. For a given distance z, this solution scales with the dimensionless parameters z/L_D, L_A/L_Δ and $\Phi_{NL} = (z/L)\cdot(L_A/L_{NL})$. Being $S(z,\omega)$ a Gaussian stationary noise, $a(z,\omega)$ is again a stationary Gaussian stochastic process, whose PSD can be obtained in a closed form.

In the DPSK modulated case, the nonlinear length L_{NL} is now a function of time, and eq. (1) does not apply. In such a case the linearization approach yields a linear time-varying approximation of the NLSE, whose solution still yields a Gaussian, but non-stationary noise. However, eq. (1) reveals that, at a specific ω, the noise field depends only on the neighboring frequency samples within a proper bandwidth, which is essentially set by L_A/L_Δ and slightly varies with the CW power P. Such a bandwidth corresponds to a finite memory window in the time domain. Hence, we expect that signal modulation adds only a small perturbation to eq. (1), which can still be used for evaluating the noise statistics at any time t by substituting the signal power $P(z,t)$ with a slowly varying, low-pass filtered version of it $P_{eff}(z,t)$, obtained by means of a windowed Fourier transform. We found that a proper filtering window is $H(\omega) = 1/\left[1+\left(L_A\omega^2/(4L_\Delta)\right)^2\right]$. Whenever PG is the main impairment to system performance, we assume that the signal has no inter-symbol interference (ISI), i.e. $P(z,t) \simeq P(0,t)$. Hence, at each sampling time t_k of a RZ-DPSK signal with sinusoidally-varying intensity profile, the noise PSD can be evaluated by solving (1), where L_{NL} is calculated with the effective power value:

$$P_{eff}(t_k) = \frac{1}{2}\left(1+H(\pi)\right)P_{peak} \quad (2)$$

where P_{peak} is the peak power, while for NRZ-DPSK P_{eff} coincides with P_{peak} (which is also the average power). By this way, the noise can be assumed as stationary for BER computation. Note that, since the noise PSD can be obtained in a closed form, our solution can then be applied to a fast BER algorithm, which avoids the computational burden of the exact method proposed in [5].

5. RESULTS AND DISCUSSION

We first tested our model by trying to replicate the experimental results in [1]. Fig. 3 shows the Q-factor penalty measured in [1] with circles and the prediction of our model (solid line) with NRZ- (left) and RZ-DPSK (right) ($d = 0.33$), for a launched power of 7 dBm. For the system parameters see [1]. For the RZ case, we plot the Q penalty obtained by using either the average P_{avg}, or the peak P_{peak}, or the effective power P_{eff} in the ASE PSD evaluation. From the comparison with experimental data, P_{eff} is found to give the best approximation. In Fig. 4 we also numerically tested our BER results obtained with P_{avg} (circles), P_{peak} (diamonds) and P_{eff} (up-triangles) and by comparing them to the exact BER (down-triangles) evaluated with the algorithm proposed in [5]. We studied a 20-span fully compensated RZ-DPSK ($d = 0.5$) system (see Fig. 1), with a GVD transmission fiber $D_{tx} = 2$ ps/nm/km, at $L_A/L_\Delta =$

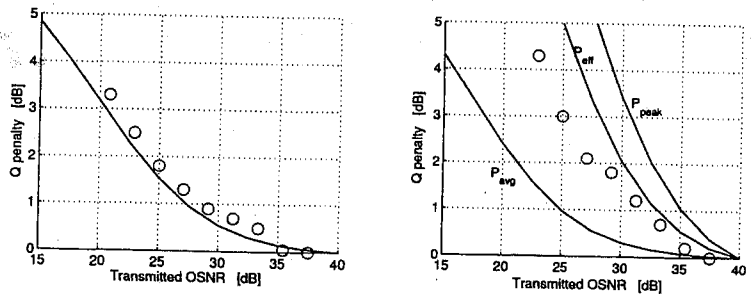

Figure 3. Q-penalty versus transmitted OSNR for NRZ- (left) and RZ-DPSK (right) for the experimental system tested in ref. [1] with a launched power of 7 dBm.

0.35 (i.e., $R = 40$ Gb/s) and for an average $\Phi_{NL} = 0.3\pi$. The best fit is given by using P_{eff}, while use of P_{avg} or P_{peak} under/overestimates the BER.

Having tested the accuracy of our model for BER calculation, we then applied it in a comparative study among NRZ- and RZ-DPSK and DQPSK system performance (see Section 2), evaluated for varying system parameters.

In Fig. 5 we plot the OSNR penalty (@BER $= 10^{-10}$) versus L_A/L_Δ for $\Phi_{NL} = 0.1\pi$ (triangles), $\Phi_{NL} = 0.3\pi$ (circles) and $\Phi_{NL} = 0.5\pi$ (diamonds) computed with (solid line) and without (dashed line) PG, for NRZ- (left) and RZ-(right) DPSK (top) and DQPSK (bottom) signals. The in-line residual dispersion is optimized with PG. In the NRZ case the performance is set by PG at low L_A/L_Δ, while self-phase modulation (SPM) induced signal distortion is dominant at high L_A/L_Δ. For this reason, the relative penalties between the curves with and without PG decrease for increasing L_A/L_Δ, in both DPSK and DQPSK case. RZ pulse coding (d=0.5) is more robust to ISI both with

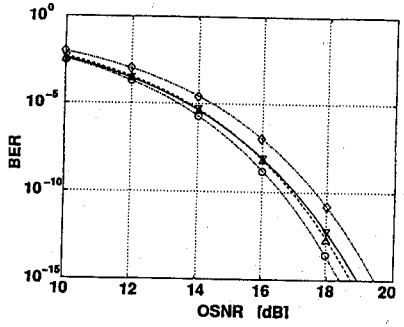

Figure 4. BER versus OSNR for a 40 Gb/s 20-span full compensated system. Triangles up: exact BER [5]. Triangles down: proposed model by using eq. (2). Circles/Diamond: proposed model with P_{av}/P_{peak}.

and without PG at high L_A/L_Δ, while at low L_A/L_Δ it has worse performance than NRZ coding [1], as expected since P_{peak} is doubled. Note that, at a fixed L_A/L_Δ, the reduced distance among the DQPSK symbols reduces its robustness to SPM distortion. In Fig. 6 we focused on the OSNR penalties plotted versus Φ_{NL} for the same system of Fig. 5, now studied for D_{tx}= 8 ps/nm/km at $R = 40$ Gb/s (L_A/L_Δ =1.4) and RZ coding. Since DQPSK supports two channels at an halved symbol rate compared to DPSK, it is found to be much less robust to PG, being PG much stronger at lower symbol rates. For the same DPSK system studied in Fig. 6, we investigated the RZ-DPSK dependence on the normalized in-line dispersion per span z/L_D. In Fig. 7 we show the contour plots of the additional OSNR penalty due to PG versus Φ_{NL} and z/L_D. Best performance is found for negative in-line dispersion, where a large tolerance to z/L_D variations is found up to $\Phi_{NL} = 0.25\pi$.

6. CONCLUSIONS

We showed that in dispersion-managed DPSK and DQPSK systems the impact of nonlinear phase noise can be studied by a parametric gain approach which describes the ASE noise with Gaussian statistics, for which we provide a simple and accurate model. Such a model is applied to BER evaluation for

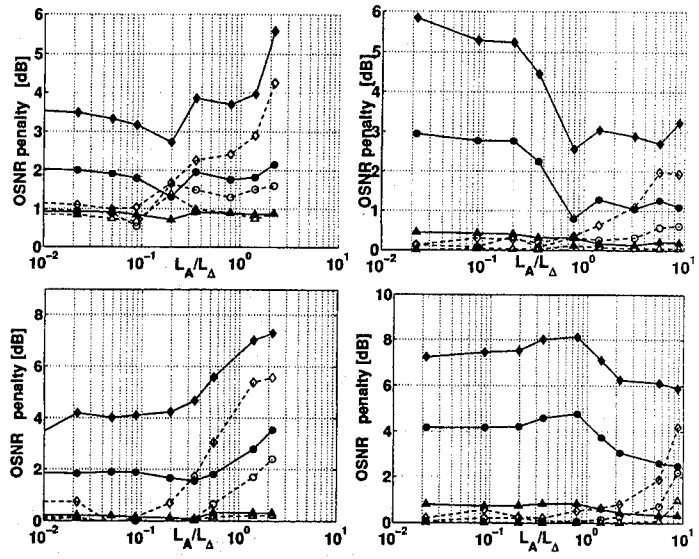

Figure 5. OSNR penalties versus L_A/L_Δ for NRZ- (left) and RZ- (right) DPSK (top) and DQPSK (bottom) modulation formats with (solid line) and without PG (dashed line). Triangles:

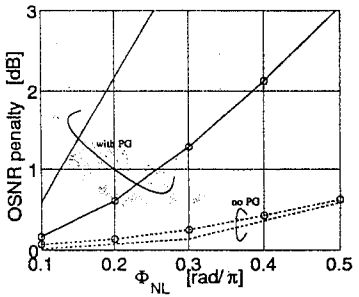

Figure 6. OSNR penalties versus Φ_{NL} for RZ-DPSK (circles) and DQPSK (no symbols) with (solid line) and without PG (dashed line) at $L_A/L_\Delta = 1.4$.

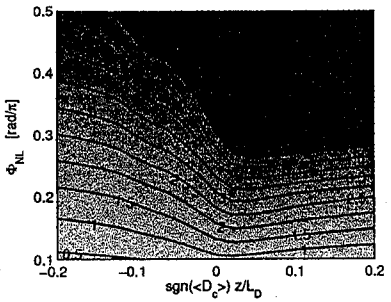

Figure 7. Additional OSNR penalties due to PG for RZ-DPSK at $L_A/L_\Delta = 1.4$ versus Φ_{NL} and $\frac{z}{L_D}$.

quadratic detectors in Gaussian noise. We found that even if RZ coding is more tolerant to SPM distortion than NRZ, it is less robust to PG, whose effect is enhanced by signal modulation. DQPSK doubles the spectral efficiency of DPSK at the price of a reduced tolerance to PG.

ACKNOWLEDGMENTS

The authors would like to thank J.-C. Antona and S. Bigo for helpful discussions and Alcatel R&I, France, for supporting this work.

REFERENCES

[1] H. Kim and A. H. Gnauck, "Experimental investigation of the performance limitation of DPSK systems due to nonlinear phase noise," *IEEE Photon. Technol. Lett.*, vol. 15, pp. 320–322, Feb. 2003.

[2] O. Vassilieva, T. Hoshida, S. Choudhary, H. Kuwahara, "Non-linear tolerant and spectrally efficient 86 Gbit/s RZ-DQPSK format for a system upgrade," in *Proc. OFC 2003*, Atlanta, GA, USA, pp. 22-24, ThE7, Mar. 2003.

[3] J.-P. Gordon and L. F. Mollenauer, "Phase noise in photonic communications systems using linear amplifiers," *Opt. Lett.*, vol. 15, no. 23, pp. 1351–1353 , Dec. 1990.

[4] K. Po-Ho, "Probability density of nonlinear phase noise," *J. Opt. Soc. Am. B*, vol. 20, pp. 1875–1879, Sep. 2003.

[5] R. Holzlohner, V. S. Grigoryan, C. R. Menyuk, and W. L. Kath, "Accurate calculation of eye diagrams and bit error rates in optical transmission systems using linearization," *J. Lightwave Technol.*, vol. 20, pp. 389–400, Mar. 2002.

[6] E. Forestieri, "Evaluating the error probability in lightwave systems with chromatic dispersion, arbitrary pulse shape and post-detection filtering," *J. Lightwave Technol.*, vol. 18, pp. 1493–1503, Nov. 2000.

[7] M. J. Ablowitz, and T. Hirooka, "Resonant intrachannel pulse interactions in dispersion-managed transmission systems," *IEEE J. Quantum Electron.*, vol. 8, pp. 603–615, May-June 2002.

CHARACTERIZATION OF INTRACHANNEL NONLINEAR DISTORTION IN ULTRA-HIGH BIT-RATE TRANSMISSION SYSTEMS

Invited Paper

Robert I. Killey, Vitaly Mikhailov, Shamil Appathurai, and Polina Bayvel
Optical Networks Group, Department of Electronic and Electrical Engineering, University College London, Torrington Place, London WC1E 7JE, UK
r.killey@ee.ucl.ac.uk

Abstract: Signal distortion due to intrachannel cross-phase modulation and four-wave-mixing limits transmission distances in ultra-high bit-rate optical communications. To gain an understanding of the effects of nonlinear pulse interactions and to quantify the effectiveness of new methods to suppress them, accurate characterization techniques are required to isolate the effects of fibre nonlinearity from the other impairments which occur in transmission. In this paper, we discuss two techniques: firstly, the direct measurements of the signal waveform distortion (pulse timing jitter, amplitude fluctuations, and FWM-induced 'ghost' pulse power) and, secondly, measurements of the BER-dependence on optical signal launch power. We describe the use of these characterization methods to investigate the suppression of nonlinear distortion through the use of optimized dispersion maps, alternate-polarization and alternate-phase return-to-zero signal formats.

Key words: dispersion management; optical fiber nonlinearity; four wave mixing; cross phase modulation.

1. INTRODUCTION

Limits to the transmission distances achievable in high bit-rate systems are imposed by nonlinear refraction. The intensity modulation of the signals induces optical phase shifts due to the intensity-dependence of the refractive index of the transmission fibres. In WDM systems with narrow channel spacing, the nonlinear refraction leads to interactions between channels through